Results in Engineering 16 (2022) 100762

Contents lists available at ScienceDirect

Results in Engineering

journal homepage: www.sciencedirect.com/journal/results-in-engineering

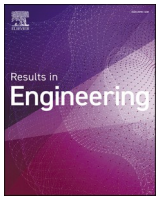

Automated feed rate optimization with consideration of angular velocity according to workpiece shape

Petr Vavruska [a,*], Matej Pesice [a], Pavel Zeman [a], Tomas Kozlok [b]

[a] Czech Technical University in Prague, Faculty of Mechanical Engineering, Department of Production Machines and Equipment, Horská 3, 128 00, Prague 2, Czech Republic
[b] TOS VARNSDORF, a.s.; Říční 1774, 407 47, Varnsdorf, Czech Republic

ARTICLE INFO

Keywords:
Feed per tooth
Optimization
Angular velocity
Toolpath
Pole of motion

ABSTRACT

Selecting the proper cutting conditions for milling parts is one of the most important tasks in setting up manufacturing to achieve minimum machining times and to ensure the desired tool life. This is particularly important when machining parts made of difficult-to-cut materials. However, if the required technological conditions are not achieved due to the shape of the toolpath itself, even the conventional setting of the technological conditions will not help achieve the optimum result. It is therefore essential to ensure that the technological conditions are achieved directly at the contact point between the tool and the workpiece, which is often forgotten in automatic toolpath preparation. This paper therefore presents a specific solution for optimizing the feed rate right at the contact point between the workpiece and the tool to maintain a constant feed per tooth. The work contributes to the investigation of the relationship between the tool diameter and the shape of the machined surface when a constant feed per tooth is required as well. The achievement of feed rate is performed by tests on the machine tool and the benefits of using the optimization of feed rate are further discussed.

1. Introduction

Some of the main directions in dynamic feed rate control research include, for example, optimization aimed at achieving a constant material removal volume, constant force load during machining, smooth spindle loading, or prevention of vibrations during machining. There are fewer papers focused on optimizing the feed rate by the shape of the toolpath itself. Other related topics deal with toolpath calculation algorithms in the machining technology preparation phase, as well as toolpath calculation directly in the control system to achieve smooth relative movement between the tool and the workpiece through adequate control of the machine tool drive parameters.

An example of one approach is the method of selecting the optimal cutting conditions during machining (spindle speed, cutting width and feed rate) presented by Sun et al. [1]. This method uses a combination of the principle of predicting the cutting forces and calculating the material removal rate per tooth and then predicting the machining errors, which must not exceed permitted values. Bediaga et al. [2] presented an automatic evaluation of cutting conditions for machining operation settings on a machine tool to prevent chatter. The proposed algorithm is capable of proposing adjustments to cutting conditions to achieve stable machining. A frequency spectrum measurement from the audio signal (using PDA) is used for this purpose. The automatically recommended cutting conditions are then taken over manually and used to modify the NC program.

Sodemann et al. [3] have shown that achieving the required feed rate is particularly important for maintaining the required accuracy in micromachining. In their work, they presented feed rate optimization based on the actual toolpath radius combined with an algorithm for suitable path segmentation. Krajnik et al. [4] presented a method that is based on the determination of the toolpath curvature radius for feed rate optimization including machine tool characteristics (such as corner acceleration) to simultaneously control the feed rate. The feed rate changes are then smooth as is the relative movement between tool and workpiece. The influence of cutting conditions, as well as the feed rate, on the resulting achievement of the desired surface roughness is presented, for example, in a study conducted by Santhosh et al. [5], which is focused on turning.

Erkorkmaz et al. [6] also include machine tool drive parameters in their proposed feed rate control optimization function. The aim is to achieve the smoothest possible feed rate changes and therefore toolpath points are replanned by approximating the points from CL data with

* Corresponding author.
E-mail address: P.Vavruska@rcmt.cvut.cz (P. Vavruska).

https://doi.org/10.1016/j.rineng.2022.100762
Received 11 August 2022; Received in revised form 1 November 2022; Accepted 9 November 2022
Available online 12 November 2022

spline curves. The machine drive limits are also reflected in the resulting feed rate value calculation. Erdim et al. [7] compared two feed rate optimization approaches (based on cutting force prediction and the volume of material removed). They theoretically and experimentally compared the two methods and concluded that their proposed feed rate optimization method based on material removal generates higher feed rate values than strategies based on cutting force predictions. Yau et al. [8] introduced the consideration of the toolpath shape and machine dynamics setup as an approach to recalculating the feed rate using NURBS curve interpolation. Feng et al. [9] presented optimization by maximizing the feed per tooth, a method based on calculating the cutting force and the allowable errors/deviations of the resulting machining using the mill geometry and the toolpath increment.

Tounsi et al. [10] presented a method of optimizing the feed rate with respect to machine tool motion dynamics at the calculated movement trajectory to achieve a nearly constant cutting force. The proposed method includes monitoring of accuracy, which is defined by the absolute deviation of the actual and theoretical target coordinate of each path segment. Using a simulation model, the resulting cutting force is determined according to this deviation, and then the optimal feed rate is calculated.

Xu et al. [11] introduced another feed rate control approach based on a model that predicts spindle performance by considering different milling methods. The goal is to achieve the lowest machining time. Rattunde et al. [12] presented a similar topic.

Xie et al. [13] used the neural network method to optimize the feed rate to achieve a smooth spindle load along the toolpath without abrupt changes during three-axis machining. Liu et al. [14] presented position-oriented process monitoring. This method is based on calculating the actual material removal rate, predicting vibrations and cutting forces during machining, and then modifying the feed rate in an NC program. The proposed method was verified experimentally by machining two thin aerospace parts (one made of aluminum alloy and the other of titanium). The optimization is based on synchronizing the sensed signals obtained directly from machining and the data regarding the tool position relative to the part from the NC program. Rahman et al. [15] presented a method involving an iterative selection of the feed per tooth based on a cutting force constraint derived from a static tool deflection mode. The feed rate and tool length changes are then used to calculate the machining time.

Mayor et al. [16] presented two toolpath segmentation method solutions leading to reduced machining time. Both of the proposed methods increase the feed rate by adjusting the distribution of toolpath points to achieve smooth motion while controlling the machine tool drives. Sarasua et al. [17] implemented a calculation of cutting forces to allow a technologist to visualize the cutting force characteristic after the toolpath calculation in the CAM system. The cutting force prediction can then be taken into account to optimize the feed rate when generating the final NC program. Tunc et al. [18] presented a method to calculate the actual contact area between the tool and the workpiece in order to predict the cutting forces and torque. The contact area is calculated based on the cutter location data, which is the direct output from the CAM system.

Budak [19] presented an advanced method of calculating cutting forces for multi-axis milling. A calculation using discrete tool elements is used as a basis for determining the material removal rate and cutting force components. At the same time, the stability diagram for several feed rate levels is determined and then the feed rate is optimized during the roughing operation. Kolar et al. [20] propose an extended model for the prediction of the quality of the machined surface by integrating the dynamics of the machine tool. This model is then used to optimize the interpolator parameter settings, thus affecting the feed rate profile during machining. The model is integrated into an application that can be used to visualize errors on the workpiece surface.

Every control system, in addition to accurately planning the toolpath, must also be able to keep the required feed rate as constant as possible, whether it is designed directly for machining or for handling objects where exceeding the required feed rate for a given part weight poses a risk of loosening the part. A conceptual design of the control system is presented, for example, by Tamayo et al. [21]. An algorithm generating a time-dependent function to recalculate the feed rate (depending on the curvature of the trajectories) was proposed by Tsai et al. [22]. In this optimization, the derivative of the time function is used to control the magnitude of the change in the feed rate during the machining operation. Zhang et al. [23] presented a feed rate control algorithm based on the smooth connection of two consecutive arcs to achieve smoothness of the tool movement. The proposed feed rate control algorithm is designed to be implemented in a control system and is therefore capable of real-time operation. Sencer et al. [24] also presented a solution based on achieving the smoothest possible tool movement. However, in this method, quintic Bézier blends with six control points are used for smooth transitions between linear toolpath movements. The advantage lies in achieving G2 continuity as opposed to other solutions, which is particularly advantageous when controlling smooth changes in the feed rate. Chen et al. [25] presented a toolpath increment scanning method (UALISM) to efficiently calculate and adjust the feed rate, especially in the inner corners of the workpiece on the toolpath. The calculation also includes the maximum defined accelerations and machine tool axis speeds. Yeh et al. [26] proposed an interpolation method using an adaptive feed rate control to reduce the toolpath control error. The non-exceedance of a specified deviation limit on linear path segments is controlled. Farouki et al. [27] presented feed rate control optimization that is dependent on the curvature of the machined surface. Pythagorean-hodograph (PH) curves were used to make the method suitable for implementation in a control system. The reduction of cutting forces during machining was verified experimentally.

Maintaining the required technological conditions at constant values is essential, especially for difficult-to-machine materials where tool wearing is rapid. Difficult-to-cut materials are nowadays very often used in additive manufacturing or hybrid technologies, where the part is first printed and then machined. Often, these are complex parts produced by wire arc additive manufacturing, often with the subsequent necessary finishing machining of the parts, as shown, for example, in the study by Li et al. [28].

An important conclusion from the analysis is that there are advanced feed rate optimization methods to maintain a constant material removal rate per tooth, maintain a constant tool load, or ensure smooth feed rate changes along the toolpath. However, the influence of the tool diameter and part contour radius parameters on the actual feed rate achieved at the actual point during machining with respect to the angular velocity of motion has not yet been investigated. Therefore, the aim of this work is to propose a solution that would optimize the feed rate according to the change in the angular velocity of the tool motion relative to the part and achieve the desired feed per tooth during machining.

2. Analysis of feed rate control with consideration of angular velocity

For the first stage of the investigation, the feed rate at the contact point can be calculated simply from the similarity of the triangles if the radius of the tool and the radius of the machined arc are known. The derived relationships are given in (1) and (2) for the inner arc (Fig. 1) and in (3) and (4) for the outer arc (Fig. 2). The feed rate at the tool center at the toolpath of radius r (offset from the workpiece by the tool radius value R_T) is marked as v_{f_TT}. The feed rate at the contact point is denoted by v_{f_CC} for the case of an inner (concave) arc and v_{f_CV} for the case of an outer (convex) arc.

An analysis of this issue shows that when milling a certain contour at a fixed tool feed rate, overloading of the tool edge can occur on certain shapes (inner corners) if the actual feed rate is too high at the contact point between the tool and the workpiece. Conversely, in some cases (on

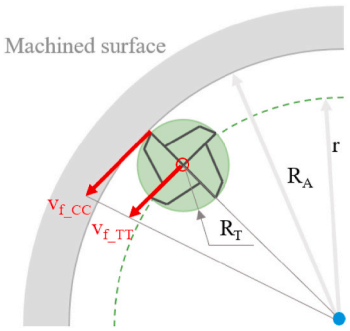

Fig. 1. Feed rates when milling inner arc.

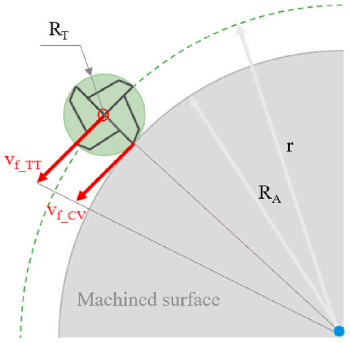

Fig. 2. Feed rates when milling outer arc.

outer corners), the potential of the tool may be unused because the current feed rate at the contact point is unnecessarily low. The main criterion taken into account is the maintenance of a constant feed per tooth at the contact point between the tool and the workpiece.

$$\frac{v_{f\_CC}}{R_A} = \frac{v_{f\_TT}}{R_A - R_T} \tag{1}$$

$$v_{f\_CC} = \frac{R_A * v_{f\_TT}}{R_A - R_T} \tag{2}$$

$$\frac{R_A}{v_{f\_CV}} = \frac{R_T + R_A}{v_{f\_TT}} \tag{3}$$

$$v_{f\_CV} = \frac{R_A * v_{f\_TT}}{R_T + R_A} \tag{4}$$

Fig. 3 shows the dependence of the feed rate at the tool-workpiece contact point on the tool radius R_T. Each line corresponds to a different radius of the machined arcs, respectively the inner and outer arcs. The horizontal line (v_{f_TT}) corresponds to the case of machining a straight section, i.e., the feed rate at the contact point remains constant regardless of the tool diameter. In the case of machining inner arcs, as the tool diameter increases on a given radius of the toolpath, the v_{f_CC} feed rate at the contact point also increases. On the other hand, in the case of outer arc machining, as the tool diameter increases at a given radius of the toolpath, the feed rate v_{f_CV} at the contact point decreases. In this case, when the toolpath radius is equal to the tool radius, the feed rate v_{f_CV} is zero. As the tool diameter increases further, the feed rate at the tool contact point becomes negative at a given toolpath radius.

Fig. 4 shows the predicted results of the sensitivity analysis (by using proposed equations) of the consideration of the angular velocity at a particular contact point, where the diameter of the machined arc is plotted on the horizontal axis and the tool feed rate value on the vertical axis. The nominal value of the feed rate of the tool center used for calculation is $v_{f\_TT} = 4000$ mm/min. The characteristics for the different tool diameters used in machining the outer and inner arcs are observed. The analysis shows that when the feed rate is set constant, the feed rate at the contact point is significantly exceeded in the case of inner radii. This can lead to overloading of the tool at that point on the toolpath and consequently reduce the tool life. In the case of the outer radius section, the feed rate change at the contact point is much lower than in the case

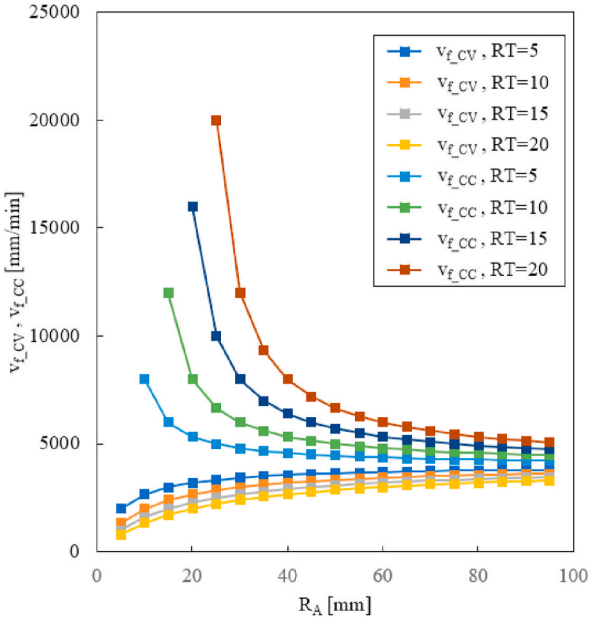

Fig. 4. Feed rate characteristics at the contact point in relation to the workpiece radius for a constant tool centre feed rate (for different tool radii R_T).

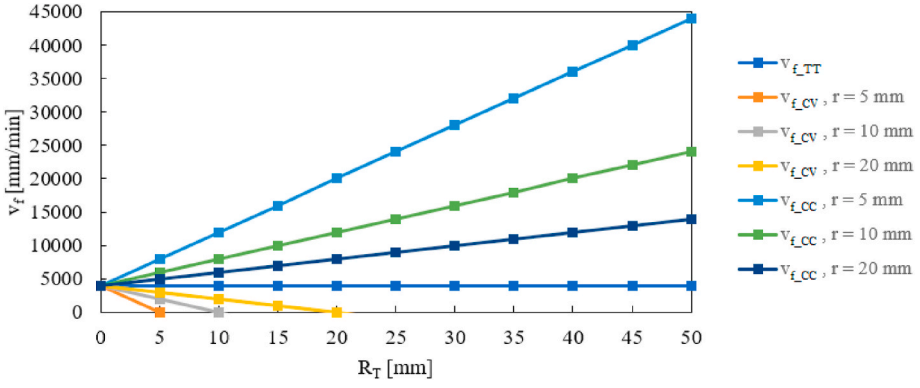

Fig. 3. Feed rate characteristics at the contact point in relation to the toolpath radius (for different tool radii R_T).

of an inner radius. However, there is still potential to optimize the magnitude of the feed rate so that the influence of angular velocity is taken into account in this case as well.

Fig. 5 shows the predicted sensitivity analysis of the magnitude of the feed rate v_{f_TT} while keeping the feed rate at the tool contact point constant by using the proposed calculations. The trend visible here is the opposite of the dependence in Fig. 4, i.e., the tool center feed rate decreases for inner arcs (marked by CC) and the tool center feed rate increases for outer arcs (marked by CV).

From the ratio of the feed rate of the tool center (v_{f_TT}) to the feed rate at the contact point (v_{f_CC} or v_{f_CV}) it is possible to determine whether it is the machining of a convex or concave arc, which can be seen in Fig. 6. Moreover, other facts are shown in this figure. If the ratio of the feed rate of the tool center to the feed rate at the contact point is equal to 1, it is machining of a straight (linear) section (the radius of the tool path r is equal to infinity). If the ratio is greater than 1, it is the machining of a convex (outer) arc; conversely, if the ratio is less than 1, it is the machining of a concave (inner) arc. In the case of machining concave arcs, the limit point is the situation where the radius of the inner arc R_{CC} is the same as the radius of the tool (D/2). In this case, the value of the feed rate v_{f_TT} is zero, since there is no circular toolpath.

3. Calculation of the actual pole of motion

In order to be able to avoid the above-mentioned issue of not maintaining the feed rate at the contact point, it is necessary to know the actual radius of the machined surface and the radius of the tool path, which is the tool movement pole. The simplest way to find the pole of motion and the local radius of the toolpath curvature is to find a circle with a defined center and radius using three points on the circle. The center of the circle can be calculated as the intersection of the axes of the sides of the triangle obtained from three points. Fig. 7 depicts the described issue of interpolation of three consecutive points with the circle.

Three arbitrary toolpath points in space P_0, P_1, P_2 are considered. The points under consideration form a triangle precisely when the points are not collinear, i.e., they do not lie on the same line. The points lie on a congruent line precisely when the vector $\vec{v_1}$ is multipled by vector $\vec{v_2}$. The vectors $\vec{v_1}$ and $\vec{v_2}$ are obtained according to (5) and (6). If the results

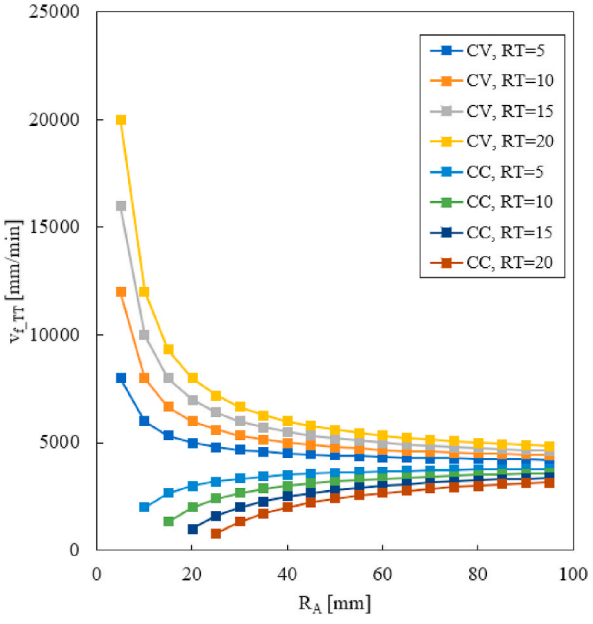

Fig. 5. The characteristics of needed tool centre feed rate (v_{f_TT}) in relation to the workpiece radius to maintain constant feed per tooth f_z at contact point (for different tool radii R_T).

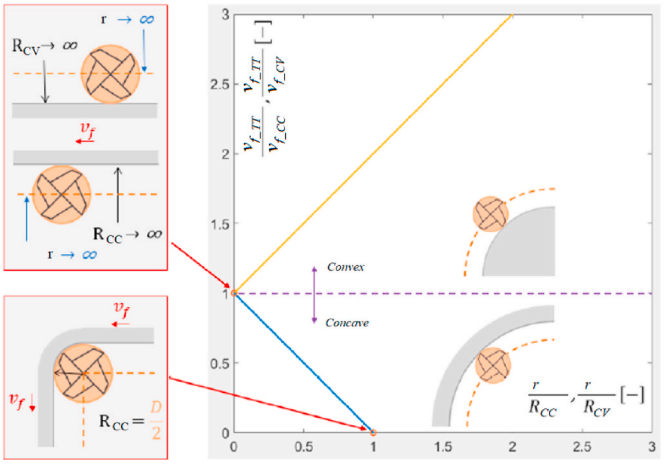

Fig. 6. Comparison of the tool centre feed rate and contact feed rate ratio, related to the ratio of the toolpath radius and worpiece radius.

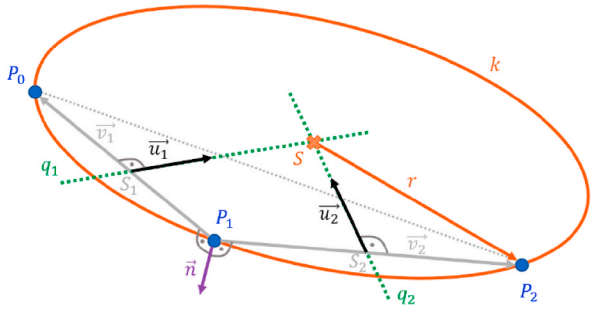

Fig. 7. Determining the pole of motion by the circle of three consecutive toolpath points.

x_1, x_2, x_3 from equations (7)–(9) are equal, then the vector $\vec{v_1}$ is multipled by the vector $\vec{v_2}$. In combination with the common point of the vectors P_1, the collinearity of the points P_0, P_1, P_2 is thus clearly proven and three such points do not form a triangle, hence there is no circle circumscribed to these points.

$$\vec{v_1} = \vec{P_1 P_0} \tag{5}$$

$$\vec{v_2} = \vec{P_1 P_2} \tag{6}$$

$$x_1 = \frac{v_{2x}}{v_{1x}} \tag{7}$$

$$x_2 = \frac{v_{2y}}{v_{1y}} \tag{8}$$

$$x_3 = \frac{v_{2z}}{v_{1z}} \tag{9}$$

In the case where the points form a triangle, the next step is to find the centers S_1 and S_2 of the segments $|P_1P_0|$ and $|P_1P_2|$ according to relations (10) and (11).

$$S_1 = \frac{P_1 + P_0}{2} \tag{10}$$

$$S_2 = \frac{P_1 + P_2}{2} \tag{11}$$

Three arbitrary points in space define a plane, in this case the plane in which the constructed circle is located. The vector product of vectors $\vec{v_1}$ and $\vec{v_2}$ from relation (12) determines the normal $\vec{n}$ (Fig. 7) of the

plane defined by points P_0, P_1, P_2, i.e., the plane also defined by vectors $\overrightarrow{v_1}$ and $\overrightarrow{v_2}$.

$$\overrightarrow{n} = \overrightarrow{v_1} \times \overrightarrow{v_2} \tag{12}$$

Vectors $\overrightarrow{u_1}$ and $\overrightarrow{u_2}$ are perpendicular vectors to the normal $\overrightarrow{n}$ and at the same time the vector $\overrightarrow{u_1}$ is perpendicular to the vector $\overrightarrow{v_1}$ and the vector $\overrightarrow{u_2}$ is perpendicular to the vector $\overrightarrow{v_2}$. Therefore, the vectors $\overrightarrow{u_1}$ and $\overrightarrow{u_2}$ can be determined to be vector products of the vectors $\overrightarrow{n}$ and $\overrightarrow{v_1}$ and $\overrightarrow{v_2}$ and $\overrightarrow{n}$ according to relations (13) and (14).

$$\overrightarrow{u_1} = \overrightarrow{n} \times \overrightarrow{v_1} \tag{13}$$

$$\overrightarrow{u_2} = \overrightarrow{v_2} \times \overrightarrow{n} \tag{14}$$

By using the points S_1, S_2 and the direction vectors $\overrightarrow{u_1}$, $\overrightarrow{u_2}$, the parametric equations (15) and (16) of the lines q_1 and q_2 (Fig. 7) are obtained.

$$q_1: \quad S = S_1 + t \bullet \overrightarrow{u_1} \tag{15}$$

$$q_2: \quad S = S_2 + s \bullet \overrightarrow{u_2} \tag{16}$$

Through the guarantee of non-collinearity of points P_0, P_1, P_2 mentioned above, the existence of the intersection S (Fig. 7) of lines q_1 and q_2 is uniquely determined. The coordinates of the intersection S are obtained by solving the system of equations (17)–(19).

$$S_{1x} + t \bullet u_{1x} = S_{2x} + s \bullet u_{2x} \tag{17}$$

$$S_{1y} + t \bullet u_{1y} = S_{2y} + s \bullet u_{2y} \tag{18}$$

$$S_{1z} + t \bullet u_{1z} = S_{2z} + s \bullet u_{2z} \tag{19}$$

Since the point S is located at the same distance from the points P_0, P_1, P_2, the distance can be evaluated to any one of the three points. For the example of calculating the toolpath radius r in relation (20), point P_2 can be selected.

$$r = |SP_2| \tag{20}$$

The disadvantage of the method of intersecting three secondary tool path points with a circle is the distortion when connecting a linear section to a circular section. The linear interpolation is uniquely determined by the collinearity of the three consecutive points. A circle intersected by such points has a radius equal to infinity. An angular velocity consideration is to be applied to the circular part of the toolpath and the feed rate of the tool center is to be adjusted to maintain its prescribed value at the contact point.

For this reason, it is necessary to introduce a condition of unambiguous determination of linear curves where the feed rate optimization should not be applied. For each of the three points intersected by the circle, the values ΔIN and ΔOUT are determined. ΔIN is the path increment between the previous and current tool tip coordinate, and ΔOUT is the path increment between the current and next tool tip coordinate. The increments ΔIN and ΔOUT are calculated by the relation for determining the distance between two points. Fig. 8 is used to illustrate an example of calculating the increments of ΔIN and ΔOUT. By substituting the coordinates P_3, P_4 and P_5 defining the circle k_4, relations (21) and (22) of the increments of ΔIN_4 and ΔOUT_4 are obtained.

$$\Delta IN_4 = |P_4P_3| \tag{21}$$

$$\Delta OUT_4 = |P_5P_4| \tag{22}$$

The values of the increments ΔIN and ΔOUT are then compared with the variable Δmax. The variable Δmax is a fixed value in the function of the minimum linear segment to which the feed rate correction should not be applied. If ΔIN is greater than Δmax, no feed rate correction will be applied to the ΔIN increment path.

It is also necessary to determine the concavity and convexity of the circle. For cases where a direct contact point between the tool and the workpiece can be obtained, the convexity or concavity of the machined curve can be determined by the distance of the point from the center of the circle.

In some cases of CAM system operations, the contact point cannot be obtained directly. Thus, for a general solution, the radius of the machined surface R_A needs to be determined in a different way, e.g., by adding or subtracting half of the tool diameter to or from the toolpath radius r. The addition or subtraction of half the tool diameter is again determined by the convexity or concavity of the machined arc. In the absence of contact point information, this is obtained by determining the position of the tool relative to the material during machining and the direction of the vector $\overrightarrow{n}$. The vector $\overrightarrow{n}$ is the normal vector of the machining plane and is determined by the vector product of the vectors $\overrightarrow{v_1}$ and $\overrightarrow{v_2}$. These vectors are generally determined by the center of the interpolating circle and the first and third points through which the circle is interpolated. The principle is explained at points P_2, P_3 and P_4 (see Fig. 9). The vectors $\overrightarrow{v_{12}}$ and $\overrightarrow{v_{22}}$ are determined according to relations (23) and (24).

$$\overrightarrow{v_{12}} = \vec{S_2P_2} = P_2 - S_2 \tag{23}$$

$$\overrightarrow{v_{22}} = \vec{S_2P_4} = P_4 - S_2 \tag{24}$$

The vector product of the vectors $\overrightarrow{v_{12}}$ and $\overrightarrow{v_{22}}$ yields the vector $\overrightarrow{n_2}$ according to relation (25).

$$\overrightarrow{n_2} = \overrightarrow{v_{12}} \times \overrightarrow{v_{22}} \tag{25}$$

Using the right-hand base rule consisting of the vectors ($\overrightarrow{v_{12}}$, $\overrightarrow{v_{22}}$, $\overrightarrow{n_2}$) and information about the position of the tool relative to the material in the cut, the convexity or concavity of the tool path can be uniquely determined.

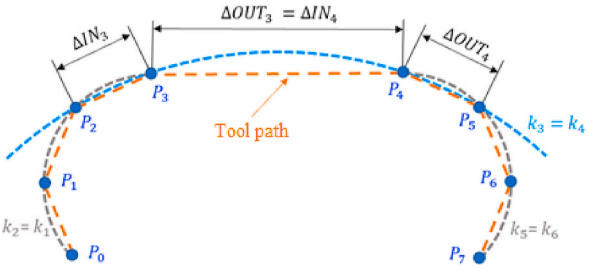

Fig. 8. Unambiguous determination of linear sections on the toolpath.

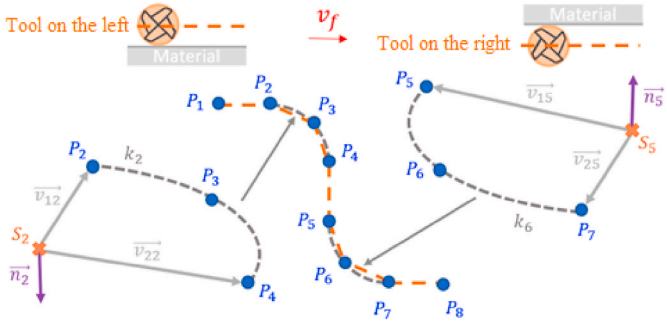

Fig. 9. Evaluation of the concavity or convexity of the toolpath depending on the defined position of the tool relative to the workpiece and the orientation of the normal $\overrightarrow{n}$

3.1. For a tool position to the left of the material

If the tool is positioned to the left of the material and the vector $\vec{n}$ is negative (pointing downwards like $\vec{n_2}$ in Fig. 9), it is a convex curve. The radius of the machined curve R_A will thus be determined according to relation (26), where R_T is the tool radius. To ensure the prescribed feed rate at the contact point between the tool and the workpiece, an increase in the feed rate is required. If the vector $\vec{n}$ is positive (pointing upwards like $\vec{n_5}$ in Fig. 9) at the same position of the tool and material, it is a concave curve (inner arc machining). The radius of the machined curve R_A will thus be determined according to relation (27). In order to ensure the prescribed feed rate at the point of contact between the tool and the workpiece, it is necessary to reduce the feed rate.

$$R_A = r + R_T \tag{26}$$

$$R_A = r - R_T \tag{27}$$

3.2. For a tool position to the right of the material

If the tool is positioned to the right of the material and the vector $\vec{n_i}$ is negative (pointing downwards like $\vec{n_2}$ in Fig. 9), it is a concave curve. The radius of the machined curve R_A will thus be calculated according to relation (27). To ensure the prescribed feed rate at the contact point between the tool and the workpiece, a reduction in the feed rate is required. If the tool is to the right of the material and the vector $\vec{n}$ is positive (pointing upwards like $\vec{n_5}$ in Fig. 9), it is a convex curve. The radius of the machined curve R_A will thus be calculated according to relation (26). To ensure the prescribed feed rate at the contact point between the tool and the workpiece, an increase in the feed rate is required.

4. Optimization algorithm proposal

The previously-mentioned calculations are used to propose the algorithm for automated feed rate optimization to achieve constant feed per tooth along the toolpath. The optimized feed rate (v_{f_opt}) is therefore calculated by multiplying the originally programmed feed rate and the ratio of two radii: the radius of the path (r) and the radius of the machined surface (R_A). In addition, it would be useful for the user to be able to adjust the maximum and minimum limits of the corrected feed rate. Therefore, the algorithm proposal includes this feature in the form of the definition of so-called feed factors (minimum and maximum), which the user can specify manually and these are then used for additional feed rate correction. To assess the feed rate limit, the ratio (v_{f_rat}) between the original feed rate (v_f) and the optimized feed rate (v_{f_opt}) is calculated. The ratio is then compared to the feed rate limit factors and if any of the limits are exceeded, then the limit factor is used to correct the feed rate. These parameters are denoted as *min_FF* (min feed factor) and *max_FF* (max feed factor) in the resulting algorithm (Fig. 10).

The proposed algorithm is implemented in the postprocessor (Fig. 11) in the form of an optimization function to be able automatically generate the NC programs. Therefore, it is not necessary for the user to make any additional action in the process of generating the NC program. CAM systems also allow the import of CL data and the display of the toolpath from the imported CL data. The color definition in the CL data can then be used to determine whether it is a rapid move, arrival, departure, or the cutting movement itself. This option can be advantageously used to visualize the characteristics of the optimized feed rate. When defining the toolpath, it is then possible to see how the feed rate would be optimized and possibly change the values of the limiting feed factors according to the specific machining case to the required range of minimum and maximum values.

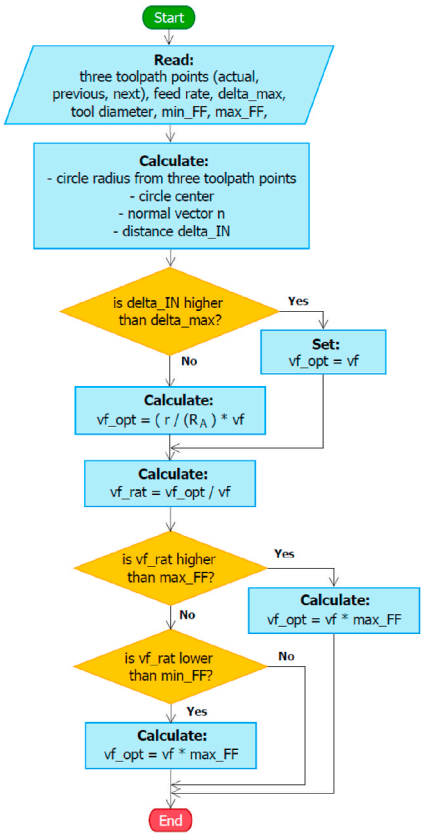

Fig. 10. Feed rate optimization algorithm flowchart.

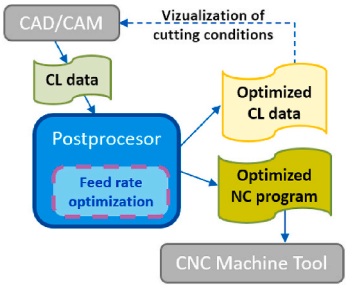

Fig. 11. Feed rate optimization imlemented into postprocessor.

5. Experimental verification

The toolpaths for milling were prepared using CAM system Siemens NX and then a simulation software [19] was used for verification purposes. Fig. 12a shows the proposed machining toolpath, where RD2 is the finishing toolpath with the conventional setup, i.e., the entire path is processed at one feed rate value. RD1 in Fig. 12b represents the finishing toolpath colored using the optimization of the feed rate (the color scale shows the magnitude of the feed rate). The curve consists of the pairs of outer and inner arcs of the same radius (20, 15, 10 and 6 mm, respectively). The section of the arcs is always of 45°. Due to the influence of angular velocity, the feed rate on the outer arc is increased by a higher value than the reduction in the feed rate on the identical inner arc. However, the toolpath on the inner arc has a shorter length than the toolpath on the corresponding outer arc, the resulting machining time for a pair of feed-optimized arcs is identical to the machining time at a constant feed rate setting.

Fig. 13 shows a comparison of the desired (planned) feed per tooth (f_z) at the contact point for the RD1 and RD2 toolpaths. From the

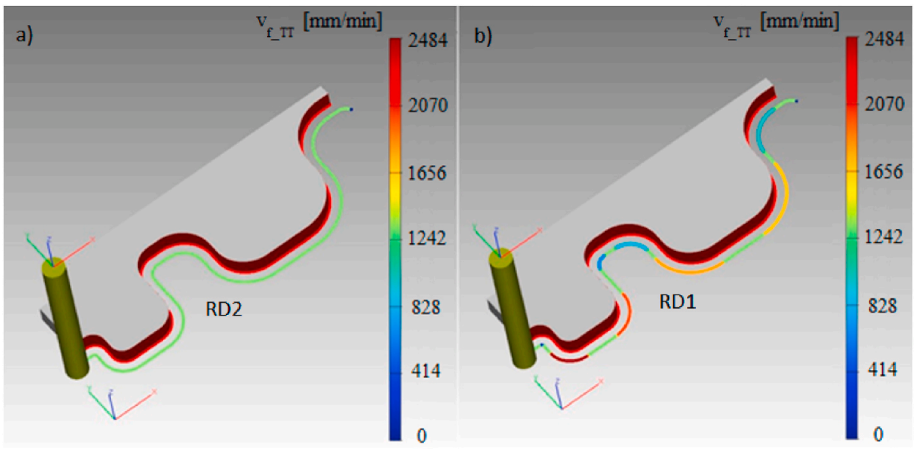

Fig. 12. Proposed toolpaths colored by feed rate value: a) - conventional setting RD2, b) - optimized setting RD1.

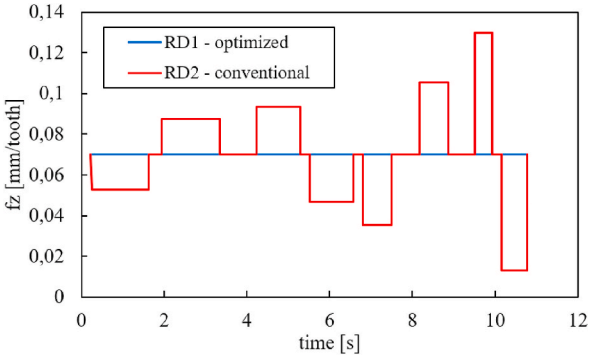

Fig. 13. Characteristics of feed per tooth.

comparison, it can be seen that in the case of the optimized path RD1, a constant feed f_z is achieved over the entire toolpath. On the other hand, on the conventional RD2 path (for fixed feed setting v_{f_TT}), the feed f_z decreases or increases on the partial sections of toolpath. When machining, it is necessary to ensure that the feed per tooth is constant, which significantly contributes to a constant cutting force. Changes in the feed per tooth, where it is higher in certain parts and lower in others, cause the tool edge to be unevenly loaded. This leads to a reduction in tool life and to non-uniform roughness of the machined surface. Therefore, the feed rate per tooth in conventional (RD2) machining is undesirable. The characteristics also show that both settings (conventional - RD2 and optimized - RD1) result in the same machining time. This occurs because paired values of the inner and outer radius of the machined contour are selected. During optimization, it is necessary to accelerate at the outer radii due to the angular velocity of the movement, whereas it is necessary to decelerate at the inner radii to achieve a constant feed per tooth. Therefore, optimization in principle reduces machine time when machining parts with outer radii, but for parts with inner radii, optimization results in an increase in machine time.

The experiment was carried out on a MCVL1000 five-axis milling center (manufacturer KOVOSVIT MAS Machine Tools) equipped with a Nikken tilt-turn table. The working space of the machine tool is: X = 1016 mm; Y = 610 mm; Z = 660 mm. The ranges of the working feed rates of all axes of the machine tool are identical: (2–12,000) mm/min. The electric spindle of the machine tool with the HSK E40 clamping interface has a maximum speed of 42,000 RPM. A six-tooth cylindrical solid carbide endmill with a nominal diameter of D = 10 mm from Iscar with the designation ECH100B22–6C10 (material grade IC900) was used as the milling tool. The cutting conditions and experimental parameters are summarized in Table 1. The clamped workpiece in the vise

Table 1
Cutting parameters.

Material	C40 steel
Cutting speed	100 m/min
Feed per tooth	0.07 mm
Axial depth of cut	15 mm
Radial depth of cut	0.1 mm
CAM Tolerance	0.006 mm

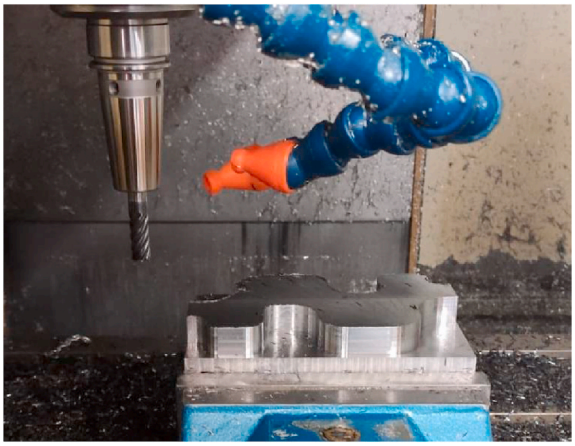

Fig. 14. Setup on machine tool.

on the machine table can be seen in Fig. 14.

6. Results and discussion

The proposed toolpaths were used for measurements performed on the machine tool. The characteristics of the programmed feed rate and achieved feed rate were obtained. Fig. 15a shows the measured feed rate characteristics using the conventional toolpath setting (constant tool center feed rate). Fig. 15b shows the measured feed rate characteristics using the toolpath with the optimized feed rate setting. Since there are always equivalent pairs of machined curve radii values, the total toolpath machining time is identical to that of the conventional setting. However, in contrast to the conventional setting (RD2) the constant feed per tooth is maintained at all points on the toolpath. The measurements also show that even when the feed rate is changed on the toolpath, there is no noticeable deviation of the achieved feed rate from the programmed feed rate.

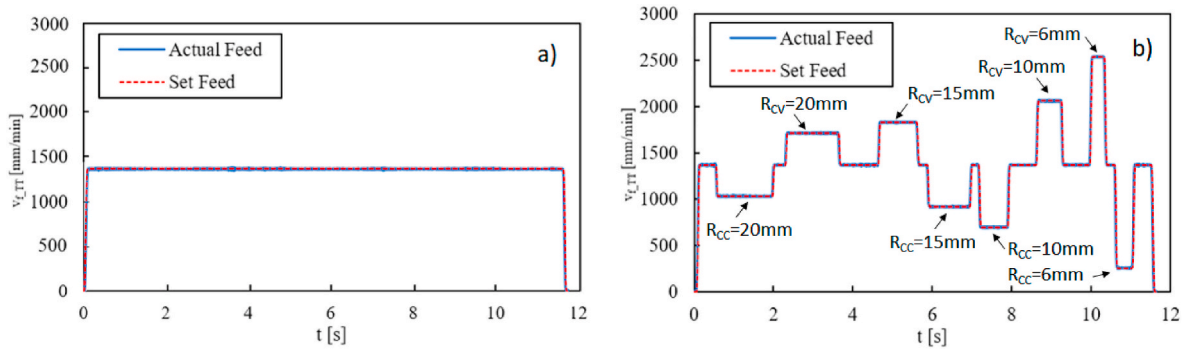

Fig. 15. Feed rate characteristics measured on the machine tool: a) - conventional setting RD2, b) – optimized setting RD1.

Table 2
Machining time comparison.

f_z [mm/tooth]	Time conventional (RD2) [min]	Time optimized (RD1) [min]
0.04	01:03.0	01:03.0
0.07	00:12.0	00:12.0
0.11	00:08.0	00:08.0
0.15	00:07.0	00:07.0

Table 2 compares the measured machining time at conventional and optimized settings for different feed rate settings of feed per tooth value. As the results show, the machining times for the conventional and for the optimized settings do not differ. This confirms the fact that the optimization increased the feed rate on the outer arcs (CV) and decreased the feed rate on the inner arcs (CC) according to the machined curve, which verified the proposed algorithm. This was clearly confirmed for different feed per tooth values. The machining time (for RD1 and RD2) is the same for this case of the toolpath because the same radius values are always used on the machined curve for the two pairs of arcs (inner and outer), as described in the first paragraph of chapter 5. In the case of the inner arc, the actual toolpath is shorter than the length of the arc itself on the part, and on this section the feed rate is always slowed down due to optimization, i.e. due to the effect of the angular velocity, so that a constant feed per tooth at the contact point is maintained. On the other hand, in the case of outer arcs, the toolpath is longer than the length of the arc itself on the curve to be machined, and in this section, thanks to optimization, i.e. the influence of the angular velocity, the feed rate is increased in order to maintain a constant feed per tooth. This also corresponds to Fig. 15b, where a decrease (for the inner arc - CC) and an increase in feed rate (for the outer arc - CV) for the equal radius values can always be seen. Therefore, due to the influence of the angular velocity in optimizing the feed rate and the actual toolpath length, the same time is achieved on all curves containing paired arcs (inner and outer) with the equal radius values as in the case of conventional machining. It also implies that there will be a significant reduction in machining time if the part contains outer arcs. However, if the part contains internal arcs, then machining time will increase.

The machined part was checked for surface quality and curve roundness using a Mahr LD130 roughness gauge with an LP C 25-15-2_90 measuring probe. In Fig. 16, the three areas in which the parameters were measured are highlighted (always on the corresponding CC and CV arcs).

6.1. Roughness and roundness measurement

The following tables show the results of the roughness parameters Ra (Table 3), Rz (Table 4) and roundness (Table 5) for the measured areas. Fig. 17 shows the comparison of surface roughness measurement results (parameter Ra), Fig. 18 the parameter Rz and Fig. 19 the resulting measured circularity at location "2" in the form of bar charts with error

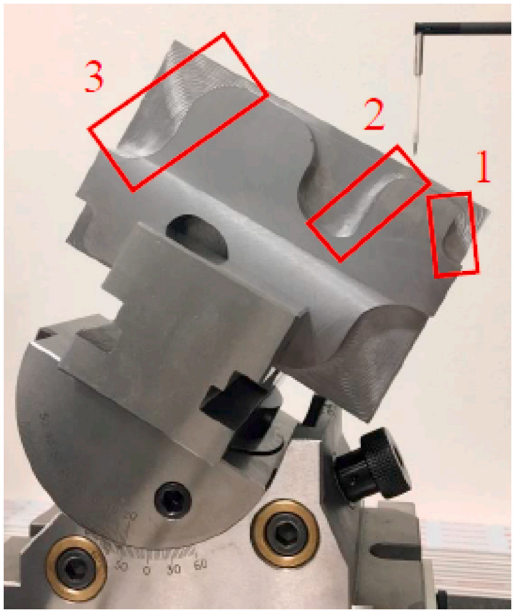

Fig. 16. Measurement of surface roughness and profile roundness.

Table 3
Ra parameter measurements.

Setting	Optimized		Conventional	
Arc type	CC	CV	CC	CV
Measured area	Ra [μm]			
1	1.45 ±0.05	1.60 ±0.06	1.87 ±0.04	1.38 ±0.05
2	1.38 ±0.05	1.52 ±0.04	1.77 ±0.04	1.24 ±0.07
3	1.3 ±0.06	1.48 ±0.06	1.72 ±0.08	1.22 ±0.06

bars. The results are very similar for the remaining two measured areas. From the results, it is clear that the surface roughness is slightly better on the inner arcs (CC) with the optimized machining setup (RD1). On the other hand, slightly better surface roughness was obtained on the outer arcs with the convential setup (RD2). The expectation that on the inner arc the maintaining feed per tooth at a constant value (i.e., local decrease of the v_{f_TT}) will improve the surface roughness is thus confirmed. But on the other hand, the maintaining feed per tooth on the outer arc (i.e., local increase of the v_{f_TT}) does not have a positive influence on the resulting surface quality. However, it is also clearly seen that after optimization, the differences between the achieved roughness

Table 4
Rz parameter measurements.

Setting	Optimized		Conventional	
Arc type	CC	CV	CC	CV
Measured area	Rz [μm]			
1	4.8 ±0.15	5.98 ±0.22	6.9 ±0.11	4.45 ±0.21
2	4.67 ±0.31	5.9 ±0.26	6.58 ±0.11	3.98 ±0.15
3	4.52 ±0.08	5.87 ±0.07	6.45 ±0.11	3.94 ±0.12

Table 5
Roundness measurements.

Setting	Optimized		Conventional	
Arc type	CC	CV	CC	CV
Measured area	Roundness [μm]			
1	90 ±3.0	65 ±4.4	77 ±5.0	88 ±5.5
2	87 ±4.7	65 ±8.9	66 ±4.4	83 ±7.9
3	95 ±6.2	70 ±6.2	72 ±4.6	93 ±9.8

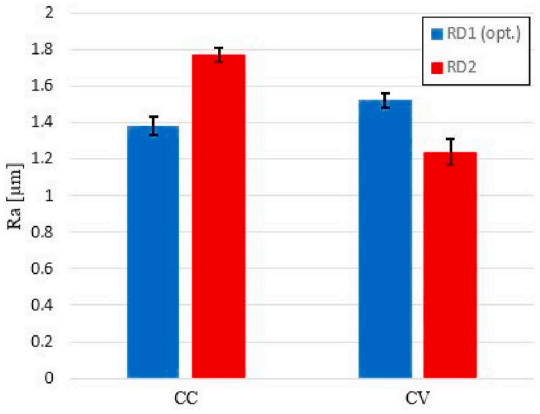

Fig. 17. Measured values of roughness parameter Ra (area "2").

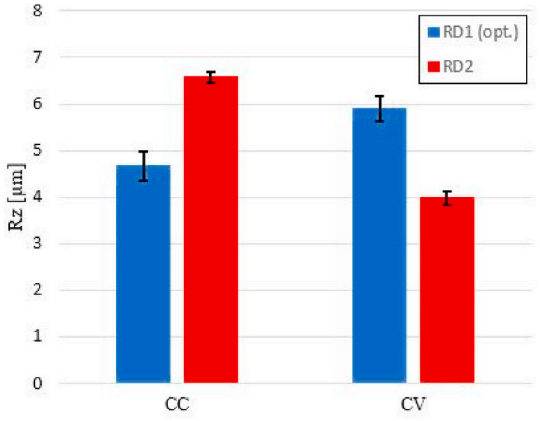

Fig. 18. Measured values of roughness parameter Rz (area "2").

value on the outer arcs compared to the roughness value on the inner arcs were reduced. In conventional machining, the differences between the roughness values on the outer and inner arcs are higher and the

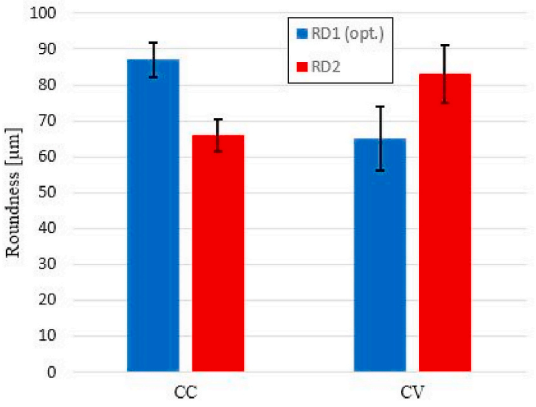

Fig. 19. Measured values of Roundness (area "2").

surface roughness is then not uniform. Therefore, the assumption that the optimization will help to obtain the uniform roughness values on the machined surface has been verified. These results may also indicate that another nominal value of feed per tooth could be found that would be optimal for this case when machining actual part from actual material with cutting tool used. The cutting conditions setup according to the tool manufacturer's recommendations was used for the milling test. The optimal value of feed per tooth can be find for the specific tool and workpiece clamping. However, finding an optimized feed per tooth value is not the focus of this paper, as the issue here is the optimization of the feed rate to maintain a certain value of constant feed per tooth. These general results can be considered to be the main conclusion regarding the influence of the optimized strategy on the resulting surface quality.

6.2. Cutting forces analysis

Achieved cutting forces were analyzed in the environment of previously verified simulation software [19], which allows both material removal simulations and cutting force predictions. The simulation software also enables to apply the flat-end mills, which are used for milling test in this paper and the computational principles used are presented by Kolar et al. [29]. The distribution of the feed rate along the toolpath in the environment of the simulation software has been shown in Fig. 12. The input parameters for the calculation of the cutting forces are the cutting conditions, material specification, and characteristics of the tool. It is necessary to specify the tool geometry parameters (helix angle 30 deg, tool length 55 mm, 6 flutes). The comparison (difference) of the cutting force magnitude for the two different approaches (conventional and optimized) is obtained. The characteristics of cutting forces based on the input cutting parameters used as well as during the test on the machine tool are seen in Fig. 20a, where the a_e (radial depth of cut) was set to the value of 0.2 mm. Differences are seen in the characteristics of cutting forces, where the conventional setup shows higher cutting forces. To enlarge the difference between the achieved cutting forces, the value of a_e was set to the value of 1 mm. The result (Fig. 20b) shows that there is a significant fluctuation in the cutting force along the toolpath when using the conventional setup (a substantial increase in cutting force in some sections). The optimized setup (RD1) shows a significantly more consistent characteristic of cutting force and does not present such high cutting force increases. This confirmed the fact that the feed per tooth has been significantly optimized to be achieved at a constant value at the most possible range along the toolpath. It can be also clarified that the differences between cutting forces achieved are higher for higher a_e values, which means that the feed rate optimization is very significant for roughing operations. However, the a_e is changing during standard roughing operations, so the constant material removal rate is needed to utilize the full potential of the optimization

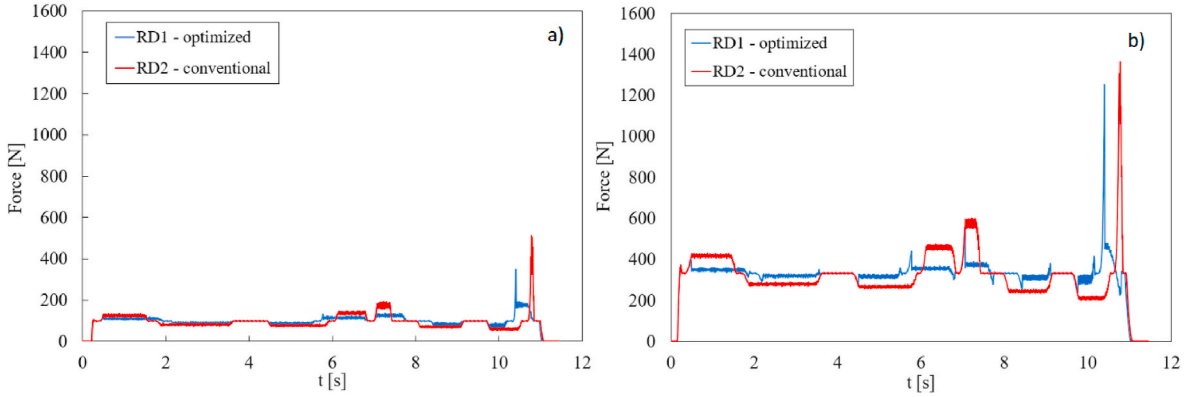

Fig. 20. Force simulation: a) $a_e = 0.2$ mm, b) $a_e = 1$ mm.

function. Nowadays so-called adaptive operations often used for roughing consist of generally curved toolpaths in order to keep the material removal rate at constant by maintaining the constant tool engagement angle. A constant material removal rate itself cannot ensure achieving of a constant feed per tooth at the contact point because of curved toolpaths. Thus, in combination with the proposed feed rate optimization, the desired cutting conditions would be fully achieved.

The proposed optimization of feed rate itself is more relevant to surface formation, which has been confirmed by the machining test and roughness measurement. Therefore the main potential to use the optimization of feed rate are finish milling applications. Standard roughing strategies are not suitable for this feed rate optimization because of variable material removal rate when milling. Nowadays so-called adaptive operations often used for roughing ensure constant material removal rate when milling and these are therefore optimal to be used in combination with the feed rate optimization. The optimization is then able to be used for finish milling as well as in roughing operations, where the main benefit can be the prolonged tool life. There are several papers that discuss this effect from different directions. Li et al. investigated, that the peak value of cutting force has a significant influence on tool life when rough milling process [30]. The importance of achieving constant cutting forces during milling is also mentioned by Wang et al. [31], who also proposed a method of smoothing the cutting force characteristic by using specifically generated toolpaths with variable radii. Balazinski et al. [32] proposed a feed rate control based on periodic waveforms to increase tool life. Lee et al. [33] presented an advanced real-time feed rate control system to achieve the optimal cutting force characteristic in relation to cutting tool wear. The importance of the effect of cutting force characteristic on tool life in high-speed machining of titanium alloy is presented by Zhang et al. al [34].

The example of a roughing toolpath based on maintaining the constant material removal rate when milling the inner section (groove) between a pair of blades can be seen in Fig. 21, where only the inner arcs occur on the toolpath. It follows that the resulting machining time will be longer when using the optimized feed rate instead of the conventional feed rate. On the other hand, the technologists can increase the feed rate, because the optimization ensures the consistent characteristic of the cutting force and the increased tool life can then be expected.

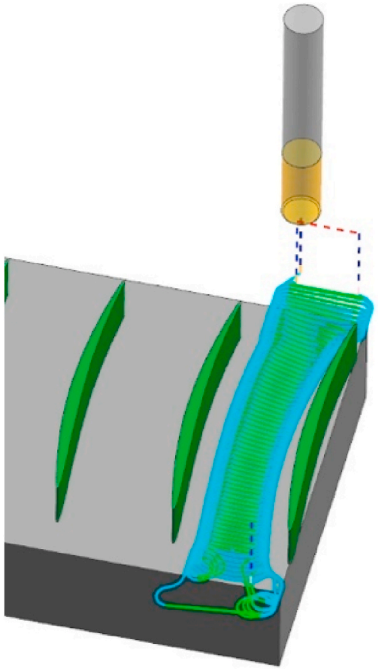

Fig. 21. Example of roughing toolpath using adaptive toolpaths (possible application of feed rate optimization).

7. Conclusion

This paper investigated the relationship between the cutting tool radius and the radius of the machined surface while achieving the desired feed per tooth value at the contact point between the tool and the workpiece. The influence of angular velocity in conventional milling causes significant changes in feed per tooth at the contact point and therefore significant tool overload occurs when machining at the inner arcs of the toolpath. This phenomenon can be avoided by using the proposed feed rate optimization method to maintain a constant feed per tooth. Thus, when machining the inner corners, lower feed rates and therefore longer machining times are achieved than in the standard case, but there is no tool overloading, i.e., excessive tool wear or even destruction. On the other hand, on the outer arcs of the toolpath, the feed rate is increased to maintain the constant feed per tooth, which reduces the machining time. The optimization method was verified by performing machining test on the machine tool and measuring of surface roughness. The assumption that the optimization will help to obtain the uniform roughness values on the machined surface has been confirmed. The proposed solution is applicable for 2D toolpaths and can be used directly when generating the NC programs by postprocessor.

Credit author statement

Petr Vavruska: Conceptualization, Methodology, Visualization, Software, Writing – original draft; Matej Pesice: Software, Data curation, Formal analysis; Pavel Zeman: Project administration, Funding acquisition, Validation; Tomas Kozlok: Writing – review & editing.

Declaration of competing interest

The authors declare the following financial interests/personal relationships which may be considered as potential competing interests: Pavel Zeman reports financial support was provided by Ministry of Education Youth and Sports of the Czech Republic.

Data availability

Data will be made available on request.

Acknowledgement

Funding support from the Czech Ministry of Education, Youth and Sports under the project CZ.02.1.01/0.0/0.0/16_026/0008404 "Machine Tools and Precision Engineering" financed by the OP RDE (ERDF). The project is also co-financed by the European Union.

References

[1] G. Sun, P. Wright, Simulation-based cutting parameter selection for ball end milling, J. Manuf. Syst. 24 (2005) 352–365, https://doi.org/10.1016/S0278-6125(05)80019-6.
[2] I. Bediaga, J. Munoa, J. Hernández, L.N. López de Lacalle, An automatic spindle speed selection strategy to obtain stability in high-speed milling, Int. J. Mach. Tool Manufact. 49 (2009) 384–394, https://doi.org/10.1016/j.ijmachtools.2008.12.003.
[3] A.A. Sodemann, J.R. Mayor, Experimental evaluation of the variable-feedrate intelligent segmentation method for high-speed, high-precision micromilling, ASME. J. Manuf. Sci. Eng. 33 (2011), 021001, https://doi.org/10.1115/1.4003010.
[4] P. Krajnik, J. Kopač, Modern machining of die and mold tools, J. Mater. Process. Technol. 157–158 (2004) 543–552, https://doi.org/10.1016/j.jmatprotec.2004.07.146.
[5] A.J. Santhosh, A.D. Tura, I.T. Jiregna, W.F. Gemechu, N.A.M. Ponnusamy, Optimization of CNC turning parameters using face centered CCD approach in RSM and ANN-genetic algorithm for AISI 4340 alloy steel, Results in Engineering 11 (2021), 100251, https://doi.org/10.1016/j.rineng.2021.100251.
[6] K. Erkorkmaz, S.E. Layegh, I. Lagozlu, H. Erdim, Feedrate optimization for freeform milling considering constraints from the feed drive system and process mechanics, CIRP Annals 62 (2013) 359–398, https://doi.org/10.1016/j.cirp.2013.03.084.
[7] H. Erdim, I. Lagozlu, B. Ozturk, Feedrate scheduling strategies for free-form surfaces, Int. J. Mach. Tool Manufact. 46 (2006) 747–757, https://doi.org/10.1016/j.ijmachtools.2005.07.036.
[8] H.T. Yau, M.J. Kuo, NURBS machining and feed rate adjustment for high-speed cutting of complex sculptured surfaces, Int. J. Prod. Res. 39 (2001) 21–41, https://doi.org/10.1080/00207540010002360.
[9] H.-Y. Feng, N. Su, Integrated tool path and feed rate optimization for the finishing machining of 3D plane surfaces, Int. J. Mach. Tool Manufact. 40 (2000) 1557–1572, https://doi.org/10.1016/S0890-6955(00)00025-0.
[10] N. Tounsi, M.A. Elbestawi, Enhancement of productivity by intelligent programming of feed rate in 3-axis milling, Mach. Sci. Technol. 5 (2001) 393–414, https://doi.org/10.1081/MST-100108622.
[11] G. Xu, J. Chen, H. Zhou, J. Yang, P. Hu, W. Dai, Multi-objective feedrate optimization method of end milling using the internal data of the CNC system, Int. J. Adv. Manuf. Technol. 101 (2019) 715–731, https://doi.org/10.1007/s00170-018-2923-8.
[12] L. Rattunde, I. Laptev, E.D. Klenske, H.-Ch Möhring, Safe optimization for feedrate scheduling of power-constrained milling processes by using Gaussian processes, Procedia CIRP 99 (2021) 127–132, https://doi.org/10.1016/j.procir.2021.03.020.
[13] J. Xie, P. Zhao, P. Hu, Y. Yin, H. Zhou, J. Chen, J. Yang, Multi-objective feed rate optimization of three-axis rough milling based on artificial neural network, Int. J. Adv. Manuf. Technol. 114 (2021) 1323–1339, https://doi.org/10.1007/s00170-021-06902-0.
[14] D. Liu, M. Luo, G.U. Pelayo, D.O. Trejo, D. Zhang, Position-oriented process monitoring in milling of thin-walled parts, J. Manuf. Syst. 60 (2021) 360–372, https://doi.org/10.1016/j.jmsy.2021.06.010.
[15] A.K.M.A. Rahman, H.Y. Feng, Effective corner machining via a constant feed rate looping tool path, Int. J. Prod. Res. 51 (2013) 1836–1851, https://doi.org/10.1080/00207543.2012.716170.
[16] J.R. Mayor, A.A. Sodemann, Intelligent tool-path segmentation for improved stability and reduced machining time in micromilling, ASME. J. Manuf. Sci. Eng 130 (2008), 031121, https://doi.org/10.1115/1.2931492.
[17] J.A. Sarasua, I. Cascon, Integration of machining mechanistic models into CAM software, Journal of Machine Engineering 14 (2014) 5–17.
[18] L.T. Tunc, E. Budak, Extraction of 5-axis milling conditions from CAM data process simulation, J. Mater. Process. Technol. 43 (2009) 538–550.
[19] E. Budak, Improving 5-axis milling operations using process models, MM Science Journal (2012) 358–364, https://doi.org/10.17973/MMSJ.2012_11_201220.
[20] P. Kolar, M. Sulitka, V. Matyska, P. Fojtu, Optimization of five-axis milling using a virtual machine tool, MM Science Journal (2019) 3534–3543, https://doi.org/10.17973/MMSJ.2019_12_2019037.
[21] E.C. Tamayo, P. Musilek, M. Al-Hussein, A.J. Qureshi, Conceptual design of controllers for automated modular construction machines, Results in Engineering 10 (2021), 100220, https://doi.org/10.1016/j.rineng.2021.100220.
[22] Y.F. Tsai, R.T. Farouki, B. Feldman, Performance analysis of CNC interpolators for time-dependent feedrates along PH curves, Comput. Aided Geomet. Des. 18 (2001) 245–265, https://doi.org/10.1016/S0167-8396(01)00029-2.
[23] D.-L. Zhang, L.-S. Zhou, Adaptation of feed rate for 3-axis CNC high-speed machining, J. Harbin Inst. Technol. 16 (2009) 391–395.
[24] B. Sencer, K. Ishizaki, E. Shamoto, A curvature optimal sharp corner smoothing algorithm for high-speed feed motion generation of NC systems along linear tool paths, Int. J. Adv. Manuf. Technol. 76 (2015) 1977–1992, https://doi.org/10.1007/s00170-014-6386-2.
[25] M. Chen, X-Ch Xi, W.-S. Zhao, H. Chen, H.-D. Liu, A universal velocity limit curve generator considering abnormal tool path geometry for CNC machine tools, J. Manuf. Syst. 44 (2017) 295–301, https://doi.org/10.1016/j.jmsy.2017.04.010.
[26] S.S. Yeh, P.L. Hsu, Adaptive-feedrate interpolation for parametric curves with a confined chord error, Comput. Aided Des. 34 (2002) 229–237, https://doi.org/10.1016/S0010-4485(01)00082-3.
[27] R.T. Farouki, J. Manjunathaiah, D. Nicholas, G.F. Yuan, S. Jee, Variable-feedrate CNC interpolators for constant material removal rates along Pythagorean-hodograph curves, Comput. Aided Des. 30 (1998) 631–640, https://doi.org/10.1016/S0010-4485(98)00020-7.
[28] Y. Li, Ch Su, J. Zhu, Comprehensive review of wire arc additive manufacturing: hardware system, physical process, monitoring, property characterization, application and future prospects, Results in Engineering 13 (2022), 100330, https://doi.org/10.1016/j.rineng.2021.100330.
[29] P. Kolar, M. Sulitka, P. Fojtů, J. Falta, J. Šindler, Cutting force modelling with a combined influence of tool wear and tool geometry, Manufacturing Technology 16 (2016) 524–531, https://doi.org/10.21062/ujep/x.2016/a/1213-2489/MT/16/3/524.
[30] H.Z. Li, H. Zeng, X.Q. Chen, An experimental study of tool wear and cutting force variation in the end milling of Inconel 718 with coated carbide inserts, J. Mater. Process. Technol. 180 (2006) 296–304, https://doi.org/10.1016/j.jmatprotec.2006.07.009.
[31] Q.H. Wang, Z.Y. Liao, Y.X. Zheng, J.R. Li, X.F. Zhou, Removal of critical regions by radius-varying trochoidal milling with constant cutting forces, Int. J. Adv. Manuf. Technol. 98 (2018) 671–685, https://doi.org/10.1007/s00170-018-2298-x.
[32] M. Balazinski, V. Songméné, L. Kops, Improvement of tool life through variable feed milling of inconel 600, CIRP Annals 44 (1995) 55–58, https://doi.org/10.1016/S0007-8506(07)62274-4.
[33] K.J. Lee, T.M. Lee, M.Y. Yang, Tool wear monitoring system for CNC end milling using a hybrid approach to cutting force regulation, Int. J. Adv. Manuf. Technol. 32 (2007) 8–17, https://doi.org/10.1007/s00170-005-0350-0.
[34] S. Zhang, J.F. Li, J. Sun, F. Jiang, Tool wear and cutting forces variation in high-speed end-milling Ti-6Al-4V alloy, Int. J. Adv. Manuf. Technol. 46 (2010) 69–78, https://doi.org/10.1007/s00170-009-2077-9.